

# Simulation of the isotropic EXAFS spectra for the S<sub>2</sub> and S<sub>3</sub> structures of the oxygen evolving complex in photosystem II

Xichen Li<sup>a</sup>, Per E. M. Siegbahn<sup>b,1</sup>, and Ulf Ryde<sup>c</sup>

<sup>a</sup>College of Chemistry, Beijing Normal University, 100875 Beijing, China; <sup>b</sup>Department of Organic Chemistry, Arrhenius Laboratory, Stockholm University, SE-106 91 Stockholm, Sweden; and <sup>c</sup>Department of Theoretical Chemistry, Chemical Center, Lund University, S-22100 Lund, Sweden

Edited by Arieh Warshel, University of Southern California, Los Angeles, CA, and approved February 20, 2015 (received for review November 18, 2014)

**Most of the main features of water oxidation in photosystem II are now well understood, including the mechanism for O–O bond formation. For the intermediate S<sub>2</sub> and S<sub>3</sub> structures there is also nearly complete agreement between quantum chemical modeling and experiments. Given the present high degree of consensus for these structures, it is of high interest to go back to previous suggestions concerning what happens in the S<sub>2</sub>–S<sub>3</sub> transition. Analyses of extended X-ray adsorption fine structure (EXAFS) experiments have indicated relatively large structural changes in this transition, with changes of distances sometimes larger than 0.3 Å and a change of topology. In contrast, our previous density functional theory (DFT)(B3LYP) calculations on a cluster model showed very small changes, less than 0.1 Å. It is here found that the DFT structures are also consistent with the EXAFS spectra for the S<sub>2</sub> and S<sub>3</sub> states within normal errors of DFT. The analysis suggests that there are severe problems in interpreting EXAFS spectra for these complicated systems.**

water oxidation | density functional theory | S-state structures | EXAFS refinement

The knowledge of the different steps of water oxidation in photosystem II has increased rapidly the past years. After the first low-resolution X-ray structures appeared ~10 y ago (1–3), quantum chemical studies using density functional theory (DFT) have played a major role for obtaining a mechanistic understanding. First, an O–O bond formation mechanism was suggested in 2006 (4) in which a terminally bound oxyl radical in the center of the oxygen evolving complex (OEC) was attacked by a manganese-bridging oxo group. Second, an improved structure was suggested in which, most importantly, the outer manganese was placed differently from where it was placed in the previous X-ray structures (5). This position led to an open space in the center of the OEC, which is critical for allowing the low-barrier O–O bond formation suggested earlier (4).

In 2011, a major experimental breakthrough occurred when the first high-resolution X-ray structure at 1.9 Å was presented by Umena et al. (6), which essentially confirmed the quantum chemical structure of the OEC. The main difference was that Asp170 was found to bind in a bridging mode between the terminal manganese and calcium instead of only terminally to the manganese as in the quantum chemical structure. The rest of the structure is very similar, including the critical positions of the outer manganese and the oxo groups, and the ligand connections. A minor problem with the X-ray structure is that it is most probably reduced by X-ray radiation (7–9), indicating that it is unlikely to be in the S<sub>1</sub> state as claimed. More recently, spectroscopic studies have played a major role by confirming the most important aspects of the quantum chemical suggestions. On the basis of the new X-ray structure and old DFT(B3LYP) structure (5), using electron paramagnetic resonance (EPR), electron nuclear double resonance (ENDOR), and DFT, a detailed structure of the OEC in the S<sub>2</sub> state was reached (10) that agrees almost perfectly with a structure obtained independently

by a DFT(B3LYP) energy minimization (11, 12) (Fig. 1). The positions of the oxo groups and the protonation states, including which ligands are water and which are hydroxides, agree, along with which manganese are Mn(III) and which are Mn(IV) at that stage. Also, the DFT(B3LYP) structure from 2009, before the high-resolution structure, is very similar (13). Two years ago, the substrate oxygen positions were suggested for S<sub>2</sub> using a W-band <sup>17</sup>O ELDOR-detected NMR spectroscopy (14). The position for the slowly exchanging substrate agrees with the one suggested by the DFT studies (4, 11–13), but there is still a minor possible disagreement for the fast-exchanging substrate. Very recently, a combined experimental and theoretical study by Cox et al. (15) used EPR and <sup>55</sup>Mn–EDNMR spectra to suggest an S<sub>3</sub> structure almost identical to the structure suggested by DFT(B3LYP) 2 y ago (16) (Fig. 2), and again very similar to the one from 2009 (13). It was claimed that only this structural model fits the measured spectra.

Even though the major features of water oxidation can now be claimed to be reasonably well understood, additional studies are required to sort out details of the mechanism. A puzzling observation stems from previous extended X-ray adsorption fine structure (EXAFS) studies of the S<sub>2</sub>–S<sub>3</sub> transition. In the EXAFS studies by Yachandra and coworkers (17–19), three short distances of 2.7–2.8 Å were found in S<sub>2</sub>. In another EXAFS study by Dau and coworkers (20), only two short Mn–Mn distances of 2.7 Å were suggested. Instead, two of the Mn–Mn distances were proposed to be longer than 3.0 Å. For the S<sub>2</sub>–S<sub>3</sub> transition, the discrepancies were even more marked. In the studies by Yachandra and coworkers (17–19), it was concluded that there is a lengthening of one of the 2.7–2.8 Å distances to

## Significance

**A few years ago, spectroscopy confirmed almost every detail of the previous density functional theory (DFT)-suggested structure for the S<sub>2</sub> state of photosynthesis. Earlier this year, the 2-y-old DFT structure for the S<sub>3</sub> state was also confirmed in detail, which means that there is now an answer to what happens in the important S<sub>2</sub>–S<sub>3</sub> transition, and there is an opportunity to discuss and evaluate the predictions for this transition made by extended X-ray adsorption fine structure (EXAFS) over the past decades. The present analysis also shows that the EXAFS spectra are consistent with the suggested DFT structures within normal DFT errors. Importantly, there are no major structural changes in this transition.**

Author contributions: P.E.M.S. designed research; X.L. and U.R. performed research; X.L., P.E.M.S., and U.R. analyzed data; and P.E.M.S. wrote the paper.

The authors declare no conflict of interest.

This article is a PNAS Direct Submission.

Freely available online through the PNAS open access option.

<sup>1</sup>To whom correspondence should be addressed. Email: ps@physto.se.

This article contains supporting information online at [www.pnas.org/lookup/suppl/doi:10.1073/pnas.1422058112/-DCSupplemental](http://www.pnas.org/lookup/suppl/doi:10.1073/pnas.1422058112/-DCSupplemental).

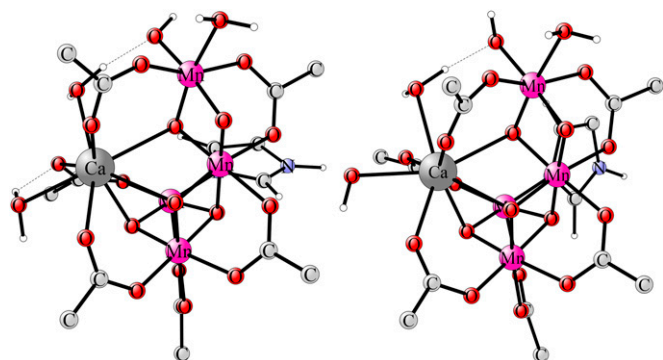


Fig. 1. (Left) Previously DFT(B3LYP)-optimized structure for the  $S_2$  state (11, 12). (Right) Structure suggested after a spectroscopic analysis (10).

3.00 Å. In the study by Dau and coworkers (20) it was instead suggested that there is a shortening of one of the distances, which was  $>3.0$  Å, down to 2.7 Å, indicating a formation of an additional Mn–Mn bis- $\mu$ -oxo bridge in  $S_3$ . Perhaps the most noteworthy of the differences of the suggested  $S_3$  distances is the one that is 2.80 Å in the Dau and coworkers (20) study, and as long as 3.0 Å in the Yachandra et al. study (17). The suggestions from both these studies give larger deviations to the DFT/spectroscopy structure than are expected from DFT, greater than 0.1 Å on some distances and a topology change. The two different EXAFS interpretations led to different proposals for the water oxidation mechanism. It should in this context be mentioned that for  $S_2$  the raw data from the two groups are the same but not for  $S_3$ . In the present work, the EXAFS information from Dau and coworkers (20) has been used. Recently, after the theoretical and spectroscopic consensus structure of  $S_2$  had appeared, a reanalysis of the EXAFS spectra was made by the group of Yachandra and coworkers (21); for the  $S_2$  structure, they now find full agreement between the EXAFS analysis and the DFT/spectroscopy structure in Fig. 1. For the  $S_3$  structure, two alternatives were given, one with essentially four equivalent distances and one where one distance is longer.

It is not straightforward to compare DFT and EXAFS data, because the latter are very sensitive to the metal–ligand distances (with an accuracy of 0.01–0.02 Å), whereas DFT calculations often give  $\sim 0.05$  Å too-long metal–O bonds and even larger deviations in the metal–metal distances. Therefore, an EXAFS

spectrum calculated directly on a DFT structure will be poor, and a direct comparison of DFT and EXAFS distances will also show extensive deviations. Instead, it is better to perform a combined EXAFS/DFT refinement of the EXAFS spectrum, in which the EXAFS raw data (not only the EXAFS distances) are used as a restraint in the DFT geometry optimization (22–24). Thereby, DFT will determine the general structure of the complex, whereas the EXAFS data will determine the detailed distances involving the metals. Such calculations are presented in this study for the  $S_2$  and  $S_3$  states, for a large DFT model used previously (11, 12), and also for a much smaller model. The results are compared with the two different experimental EXAFS analyses. The main purpose of the present study is to investigate whether the discrepancies to experiments for the computational model, concerning the structural changes in  $S_2$  to  $S_3$ , really indicate significant differences in the structures or if they are mainly due to minor differences in bond lengths and technical differences in how the spectra are analyzed. The present study agrees with earlier ones (25, 26) in that a major problem of interpreting EXAFS spectra of complicated molecules is that it is possible to fit several different structures to the same spectrum.

It should finally be emphasized that a comparison with other theoretical and experimental work is not part of the purpose of the present paper, which is instead focused on EXAFS results. However, other theoretical work on water oxidation in photosystem II has been discussed in detail in recent reviews (12, 27, 28).

## Methods and Models

In previous studies where the present starting structures were obtained, the DFT method used was the hybrid functional B3LYP (29) with the lacvp\* basis set. For the present EXAFS refinement analysis, the nonhybrid functional BP86 (30) has been used instead for technical reasons. The structures were therefore first reoptimized with this functional using a def2-SV(P) basis set. BP86 is known to give structures of similar quality as B3LYP, and the structural changes were indeed small. It has previously been emphasized that for the present system, B3LYP gives much better energetics than BP86 (31). However, the comparison made concerned relative energies for different structures, whereas in the present study the energy differences entering the fitting procedure concern points in the same local minima. Because the equilibrium geometries are very similar using B3LYP and BP86, these energy differences should also be very similar. The cluster-type modeling of the active site was used (28). The details, which are the same as used in previous studies (12), are described in *SI Appendix*.

The DFT/EXAFS refinements were performed with the ComQum-EXAFS software (23, 24). This method is a combination of QM geometry optimization and an EXAFS structure refinement, and is the same used in previous studies (22–24). Technical details are provided in *SI Appendix*.

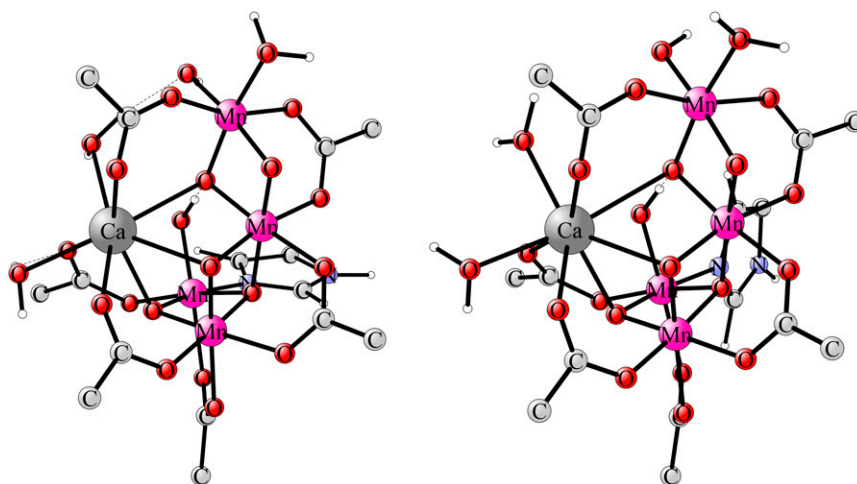


Fig. 2. (Left) Previously DFT(B3LYP)-optimized structure for the  $S_3$  state (12, 16). (Right) Structure suggested after a spectroscopic analysis (15).

## Results

The results from the present optimizations and refinements for the  $S_2$  and  $S_3$  states are given in Table 1, where the results from the experimental EXAFS analyses are also shown. For the  $S_3$  states, results for two topologically different structures are given (Fig. 3), the first ones for the energetically optimal structure with the central oxo group closer to the outer manganese Mn4, and the second for a local minimum where this oxo group is closer to Mn1. These two types of structures have been known to be nearly degenerate (“outer” oxo preferred) for the  $S_2$  state (13), and recently they have been shown to correspond to the two states observed by EPR (32). The refined  $S_3$  spectrum for the outer oxo position is shown in Fig. 4 together with the one for the  $S_2$  state. The refined spectra are superimposed in *SI Appendix*, Fig. S2. The spectrum for the “inner” oxo position is shown in *SI Appendix*, Fig. S3. The optimized distances for the  $S_2$  state from the previous study (12) using the large model were Mn1–Mn2 = 2.83 Å, Mn2–Mn3 = 2.80 Å, Mn3–Mn4 = 2.74 Å, and Mn1–Mn3 = 3.46 Å. These results were obtained using B3LYP with the lacvp\* basis set. For the present study, a reoptimization using BP86 was done. The differences to the B3LYP results are very small (0.01–0.04 Å), with the BP86 results being Mn1–Mn2 = 2.87 Å, Mn2–Mn3 = 2.81 Å, Mn3–Mn4 = 2.77 Å, and Mn1–Mn3 = 3.44 Å. The calculated results compare very well with the EXAFS analysis by Yachandra and coworkers (17), where the distances were suggested to be two of 2.73 Å, one of 2.82 Å, and one of 3.30 Å. It should be noted that the EXAFS analysis could not distinguish between the different Mn–Mn distances. In the more recent study, the results of the analysis are similar with three distances of 2.7 Å and one with 3.2 Å (21). As usual, the DFT(B3LYP) distances are somewhat long. In contrast, the EXAFS analysis by Dau and coworkers (20) suggests one distance of 2.69 Å, one of 2.74 Å and two distances larger than 3.0 Å. From the nearly perfect agreement between the general DFT structure and recent results of EPR and ENDOR spectroscopy for the  $S_2$  state (10), it must be concluded that the assignment by Dau and coworkers of only two short Mn–Mn distances is unlikely to be correct.

**Table 1. Mn–Mn distances obtained for  $S_2$  and  $S_3$  using different methods and models**

Method	Mn1–Mn2	Mn2–Mn3	Mn3–Mn4	Mn1–Mn3	Ref.
$S_2$					
EXAFS	2.82	2.73	2.73	3.30	(17)
EXAFS	2.70	2.70	2.70	3.20	(21)
EXAFS	2.69	2.74	>3.0	>3.0	(20)
B3LYP	2.83	2.80	2.74	3.46	(12)
BP86	2.87	2.81	2.77	3.44	
Refined <sup>†</sup>	2.83	2.74	2.68	3.62	
Truncated, refined <sup>‡</sup>	2.74	2.83	2.69	3.60	
$S_3$					
EXAFS	2.73	2.80	3.00	3.30	(17)
EXAFS	2.70	2.70	3.2 (2.8)	2.80	(21)
EXAFS	2.73	2.73	2.77	>3.0	(20)
Outer oxo					
B3LYP	2.84	2.81	2.76	3.55	(12)
BP86	2.88	2.82	2.79	3.53	
Refined <sup>§</sup>	2.74	2.73	2.81	3.78	
Truncated, refined <sup>¶</sup>	2.72	2.79	2.79	3.80	
Inner oxo					
B3LYP	2.75	2.78	3.18	2.89	
BP86	2.78	2.80	3.19	2.92	
Refined <sup>#</sup>	2.72	2.75	3.15	2.81	

<sup>†</sup> $\chi^2 = 337$ ; <sup>‡</sup> $\chi^2 = 169$ ; <sup>§</sup> $\chi^2 = 174$ ; <sup>¶</sup> $\chi^2 = 73$ ; and <sup>#</sup> $\chi^2 = 169$ .

The DFT/EXAFS refinement leads to the expected shortening of the three short Mn–Mn distances. The refined results are Mn1–Mn2 = 2.83 Å, Mn2–Mn3 = 2.74 Å, Mn3–Mn4 = 2.68 Å, and Mn1–Mn3 = 3.62 Å. The three short distances are now in even better agreement with the analysis by Yachandra et al. For the long Mn–Mn distance, the refined distance is slightly longer than the experimental one, but this cannot be regarded as a serious difference because this distance is extremely sensitive to details in the models used in the calculations.

Turning to the results for the  $S_3$  state, the B3LYP distances for the energetically optimal outer position of the oxo group are Mn1–Mn2 = 2.84 Å, Mn2–Mn3 = 2.81 Å, Mn3–Mn4 = 2.76 Å, and Mn1–Mn3 = 3.55 Å. The differences to the short  $S_2$  distances are +0.01 Å, +0.01 Å, and +0.02 Å, respectively. The similarity of these Mn–Mn distances to the ones for the  $S_2$  state is surprising from two aspects. First, both EXAFS studies suggest much larger changes of these Mn–Mn distances. Second, because Mn1 is oxidized from Mn(III) to Mn(IV) in this transition, there is a loss of a Jahn–Teller axis, which leads to a significant shortening of a Mn–O bond along this axis by as much as 0.6 Å, from 2.4 to 1.8 Å, though this does not seem to affect the Mn–Mn distances. The reoptimized BP86 distances show the same tendency with Mn1–Mn2 = 2.88 Å, Mn2–Mn3 = 2.82 Å, Mn3–Mn4 = 2.79 Å, and Mn1–Mn3 = 3.53 Å. The differences to the short  $S_2$  distances are +0.01 Å, +0.01 Å, and +0.02 Å, respectively, the same differences as for B3LYP. The DFT/EXAFS refinement changes the picture somewhat, with distances of Mn1–Mn2 = 2.74 Å, Mn2–Mn3 = 2.73 Å, Mn3–Mn4 = 2.81 Å, and Mn1–Mn3 = 3.78 Å, leading to differences for the short distances of –0.09 Å, –0.01 Å, and +0.13 Å, respectively, compared with the  $S_2$  distances, instead indicating two notable changes of the short Mn–Mn distances. An even larger difference is found for the long distance after the refinement, from 3.62 to 3.78 Å. However, in this context the long distance is much more sensitive to details of the structures.

The EXAFS analysis by Yachandra and coworkers (17) led to suggested distances for the  $S_3$  state of 2.73 Å, 2.80 Å, 3.00 Å, and 3.30 Å. There is one rather large difference to the DFT(B3LYP) results and this is the 3.00 Å distance, which is only 2.81 Å using DFT/EXAFS. As mentioned previously, DFT(B3LYP) normally overestimates distances, so this would be a surprising difference. In the EXAFS analysis by Dau and coworkers, the suggested distances are two of 2.73 Å, one of 2.77 Å, and one larger than 3.00 Å. Notably, the longest of the short distances is only 2.77 Å in comparison with 3.00 Å in the analysis by Yachandra et al. However, the results of the Dau and coworkers analysis are well in line with the DFT results. Again, the EXAFS raw data from the two experimental studies is different for the  $S_3$  state, and the raw data from Dau and coworkers was used here. In the recent reanalysis by the Yachandra group, two alternatives were given, one where all four distances are short, and one where one distance is longer (21). For the first of these suggestions there is thus a discrepancy to the present analysis; in the second one there is a discrepancy concerning which distance is the long one (see below).

From the above, it can be concluded that the agreement between the DFT(B3LYP) and EXAFS results are quite good compared with the Yachandra and coworkers (17) analysis for the  $S_2$  state. For the  $S_3$  state, the agreement is quite good compared with the Dau and coworkers analysis. For the earlier analysis of Yachandra and coworkers (17), the agreement is not as good. In the more recent reanalysis, there are still disagreements (see below) (21). Because the two EXAFS analyses differ substantially to each other for each state, the discrepancies between the results of DFT(B3LYP) and EXAFS become more pronounced when the changes of the distances between  $S_2$  and  $S_3$  are compared. The DFT changes of the short Mn–Mn distances



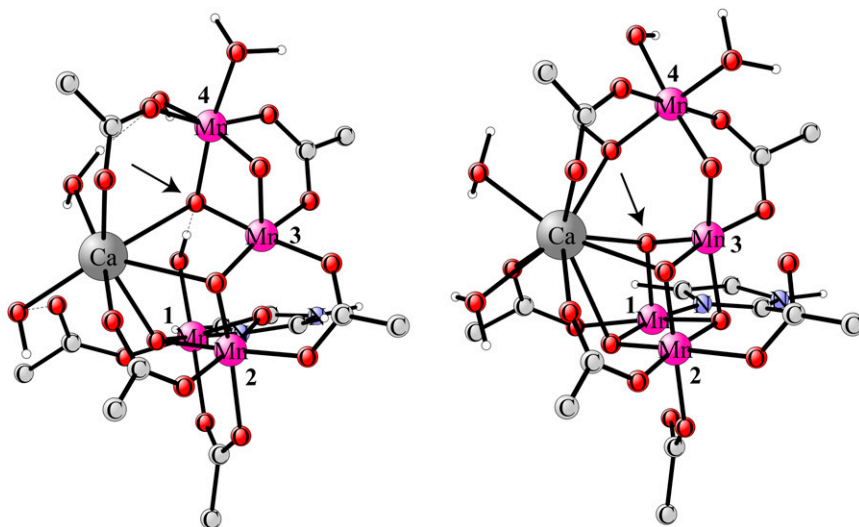


Fig. 3. The two topologically different  $S_3$  states discussed in the text, the outer oxo position (Left) and the inner one (Right).

are very small, as noted previously. However, it is interesting that the DFT/EXAFS refinement led to somewhat larger changes of  $+0.13$  and  $-0.09$  Å for two distances. The refined results therefore agree better qualitatively with the interpretations of the EXAFS studies, indicating some structural changes in this transition. A conclusion that appears clear is that DFT (B3LYP or BP86) by itself is not accurate enough for predicting the detailed changes in the distances (see below). Two of the distances (Mn1–Mn2 and Mn2–Mn3 in the cube) show the same type of shortening of the (short) distances after refinement as in the case of the  $S_2$  state, which is in line with previous experience. However, the third distance (Mn3–Mn4) to the outside manganese shows an unexpected lengthening, which may be a sign of a slightly worse description by DFT(B3LYP) for the  $S_3$  state. Errors of  $0.1$  Å are not unusual for DFT-optimized geometries. The typical accuracy of DFT calculations for metal–ligand distances is  $\sim 0.06$  Å, whereas the accuracy of DFT(B3LYP) is lower for nonbonded distances such as Mn–Mn and Mn–Ca (probably  $0.1$ – $0.2$  Å).

Even though the two experimental EXAFS analyses agree that there should be a significant structural change in the  $S_2$ – $S_3$  transition, the details of this change, and the consequences of it, are quite different in the two studies. The earlier analysis by Yachandra and coworkers (17) gave one change of more than  $0.2$  Å (or one of  $0.2$  and one of  $0.1$  Å). This change, supported by results of earlier and later XANES spectra (33), led to the conclusion that an oxygen rather than a manganese is oxidized in this transition, which strongly affected the suggested O–O bond formation mechanism (34, 35). The conclusion from the XANES spectra has been questioned experimentally (36), and also recently on the basis of DFT model calculations (37). The Dau and coworkers results, however, gave one change from a distance larger than  $3.0$  Å down to  $2.77$  Å; this led to a suggested structural change in this transition with a formation of an additional Mn–Mn bis- $\mu$ -oxo bridge in  $S_3$  (38). With the present knowledge, both from model calculations and spectroscopy experiments, none of these suggestions are likely to be correct. One conclusion that can be drawn is that it appears to be very difficult to obtain detailed structural information from EXAFS spectra, even if these are accurately measured, of such a complicated multimetal complex like the OEC, without detailed information from similar model complexes where the structures are known. Such information is presently missing.

There are two different alternatives to explain the changes of the short Mn–Mn distances that are implicated by the DFT/EXAFS refinement, assuming that it is reliable. These changes

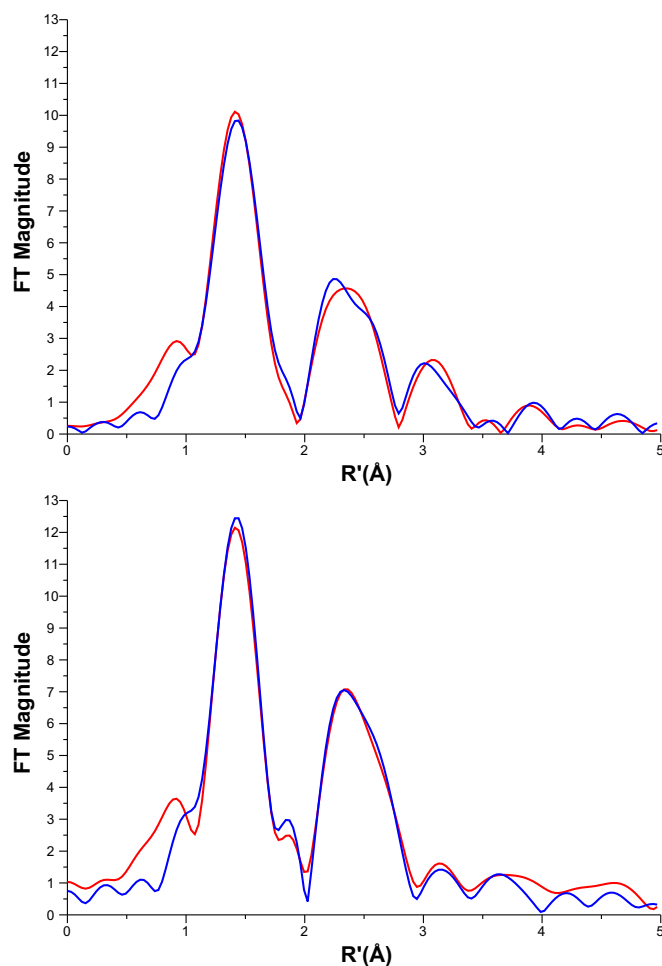


Fig. 4. (Upper) Refined EXAFS spectrum for the  $S_2$  state. (Lower)  $S_3$  state, for the case with the central oxo close to the outer manganese Mn4, the outer oxo position. Experimental spectra are in red.

could stem from either a minor error in DFT or something missing in the chemical model used. Even before the recent spectroscopic verification of also the  $S_3$  state (15) (when the present study was performed), the first possibility appeared to be by far the most likely explanation. One interesting aspect is that in this transition a strong hydrogen bond is introduced from the substrate hydroxyl group bound to Mn1 and an oxo group bridging Mn3–Mn4. The hydrogen bond is very short, only 1.49 Å, and a lengthening effect on the Mn3–Mn4 bond could have been expected, but the DFT(B3LYP)-optimized structure shows only a small lengthening of +0.02 Å; the EXAFS refinement indicates that it should be larger with +0.13 Å. The actual error for the DFT bond distances implied by the refinement is +0.06 Å for one distance and –0.05 Å for the other. DFT errors like these cannot be excluded. At the same time, Mn1 is oxidized, which could implicate a shortening of the Mn1–Mn2 bond distance. Instead, DFT surprisingly shows a small increase by 0.01 Å. The EXAFS refinement shows the expected trend with a shortening of –0.09 Å with individual errors of +0.00 Å and +0.10 Å. Again, a DFT error of this size cannot be excluded.

The second alternative to explain the effects on the distances from the DFT/EXAFS refinement would be some sort of error in the model used for the DFT calculations. Because there is a very large degree of consensus between computational modeling and spectroscopic experiments concerning both the  $S_2$  (10) and the  $S_3$  structure (15), an error of this type appears highly unlikely. Another question in that case is what type of defect this could be. An effect from the surrounding, not included in the DFT model, can most likely be ruled out on the basis of previous experience. Inside the model, a protonation of one of the  $\mu$ -oxo bonds between Mn3 and Mn4 could explain the lengthening of this bond distance, but could hardly explain the shortening of the Mn1–Mn2 bond. A protonation of an oxo bond in the  $S_2$  state is unlikely on the basis of the present knowledge of this state. In the  $S_2$ – $S_3$  transition, a water binds to the OEC and a proton from that water could, in principle, protonate one of the oxo bonds, but this would require a lack of proton release in this transition. However, there is convincing experimental evidence that a proton release does occur (38). A protonation of a  $\mu$ -oxo bond in the  $S_2$ – $S_3$  transition would furthermore complicate O–O bond formation substantially. In all known mechanisms for O–O bond formation, natural or biomimetic, an oxygen radical is critically needed. At the stage the oxygen radical is formed, the presence of another protonated group than a substrate should therefore preferably be avoided, because that group could be deprotonated instead.

Another alternative to the present optimal  $S_3$  structure could have been the one where the central oxo group is close to Mn1 (Fig. 3); this has been suggested in one of the alternatives in the recent reanalysis of the EXAFS spectra (21), but this analysis used a definition of the outer structure with a 5-coordinated Mn4 (present numbering) in contrast to the structure here. Also, it can now be added that the inner structure was ruled out by the recent spectroscopic analysis (15). The B3LYP distances (Table 1) with the energetically less optimal inner position for the oxo group are Mn1–Mn2 = 2.75 Å, Mn2–Mn3 = 2.78 Å, Mn3–Mn4 = 3.18 Å, and Mn1–Mn3 = 2.89 Å. Because EXAFS cannot identify which Mn–Mn distance is which, a comparison with the  $S_2$  distances should be made with a rearrangement of the assignments for the bonds. The differences to the short  $S_2$  distances are then +0.01 Å, –0.02 Å, and +0.06 Å, respectively. These changes are again, like for the outer model, smaller than the suggestions made by EXAFS. For the refined distances the corresponding differences are +0.04 Å, +0.01 Å, and –0.02 Å, which thus show even smaller differences to the ones in the  $S_2$  state; this is different from the case of the “outer” oxo where the refined distance changes showed a better correspondence with EXAFS. However, the results for the outer and inner structures show too-

small differences between each other to allow any conclusion of which structure should be best, on the basis of the EXAFS analysis. Energetically, the outer minimum is preferred with a margin of 4.9 kcal/mol at the B3LYP level. In line with the excellent agreement obtained so far between the DFT results and spectroscopic experiments, the suggestion based solely on the calculations would therefore be that the outer minimum is the actually preferred one; e.g., it has in this context been shown that the correct order, with a reasonable energy separation, compared with experiments, is obtained by DFT for the corresponding states in  $S_2$  (13, 32). At the BP86 level, the preference for the outer minimum is even larger by another 5 kcal/mol. As discussed, the choice between these minima does not have any major effects on the actual O–O bond formation mechanism (13). The refined spectrum for the inner oxo position is shown in *SI Appendix*, Fig. S3.

Another comment can be made concerning the present EXAFS analysis. Both the experimental EXAFS spectra show large differences between the  $S_2$  and  $S_3$  states, which was the reason for suggesting a much larger structural change than found both here and in the recent EPR spectroscopic analysis. However, the present analysis shows that it is indeed possible to obtain different EXAFS spectra for two structures with highly similar Mn–Mn distances (Fig. 4).

A remaining question is whether the DFT/EXAFS refined distances would have significant effects on the energetics, and thereby the mechanism. To test this possibility, the  $S_2$  and  $S_3$  structures were reoptimized, keeping the short Mn–Mn distances fixed to the values obtained after the refinement; by definition, this is less optimal energetically for DFT, but the difference for  $S_2$  is small, with an energy increase of only 1.3 kcal/mol. The same small difference of 1.3 kcal/mol is found for the inner minimum of  $S_3$ . For the outer minimum of  $S_3$ , the effect is slightly larger with 2.2 kcal/mol. In line with previous experience, the other detailed differences in the geometries do not matter much. Previously, it has been shown that the choice of basis set for the geometry optimization does not have significant effects on the energetics, even though this could change the distances by even more than the difference between the optimal and refined structures discussed here (39). Finally, the energies were calculated with fixed distances from the different EXAFS studies (17, 20, 21). Again the energy differences to the optimized structures are small, in the range 1–2 kcal/mol. The exceptions are when EXAFS has suggested only two, rather than three, short distances, where the energy difference goes up to 10 kcal/mol. For the most recent EXAFS study, the energy differences are also somewhat larger with 4–5 kcal/mol for the outer oxo structures. It is not possible to draw any conclusion from these values, except that the energies are insensitive to the details of the Mn–Mn distances, and these details do not affect the mechanism.

Results for a truncated model (*Methods and Models*) are also shown in Table 1. In general, the full and the truncated structures are similar. Concerning the changes of the distances from  $S_2$  to  $S_3$ , the truncated model gives a shortening (after refinement) of –0.04 Å for Mn2–Mn3, whereas the full model gives –0.01 Å. The lengthening of the distance to the outer manganese (Mn3–Mn4) is also similar in the two models with +0.10 and +0.13 Å, respectively.

## Conclusions

In the present study, a DFT/EXAFS refinement procedure has been applied to DFT structures for the  $S_2$  and  $S_3$  states, previously presented (12). Previous experimental spectroscopic studies have confirmed the details of the DFT(B3LYP) structure for the  $S_2$  state (10) (Fig. 1). Very recently (after the present study was made), a similar confirmation also exists for the  $S_3$  state (15) (Fig. 2). The oxidation states of the four manganese atoms, the ligation of the amino acids, the identification of oxo,

hydroxide, and water ligands have for both states been confirmed by the experiments. Also, the mechanism for O–O bond formation has been essentially confirmed by experiments (14). With this background it was now of high interest to go back to the analysis of the EXAFS spectra. Over many years, EXAFS studies have been made on the OEC, mainly by two groups reaching rather different conclusions. However, both groups have agreed that there should be a significant structural change in the S<sub>2</sub>–S<sub>3</sub> transition, because the EXAFS spectra for the two states are different. However, the details of this change have been suggested to be quite different. In one of the studies, a major lengthening of one Mn–Mn distance by more than +0.2 Å was suggested (17–19), whereas in the other one a major shortening of one distance by at least –0.2 Å was instead suggested (20). In contrast, the DFT(B3LYP) optimizations showed only limited changes of the Mn–Mn distances in this transition (12). The main purpose of the present study was therefore to investigate whether the DFT structures could be considered consistent with the EXAFS spectra. The conclusion from the study is that the DFT structures could be well-fitted to match the spectra keeping the same topological structures and with only minor distortions, within the normal errors of DFT; this also means that it is indeed possible to obtain EXAFS spectra that

agree very well with those obtained experimentally, even from structures of the S<sub>2</sub> and S<sub>3</sub> states that are highly similar.

The DFT/EXAFS refinement modified the previous DFT (B3LYP) results somewhat. Instead of the small changes in the S<sub>2</sub>–S<sub>3</sub> transition obtained previously, one Mn–Mn distance was suggested to increase by +0.13 Å, whereas another decreased by –0.09 Å. The most likely explanation for this correction is minor errors in DFT. Errors in metal–metal distances of this magnitude have been noticed several times before, and the energetic consequence of these errors is minor. Defects in the chemical model used are considered much less likely, in particular after the recent spectroscopic verification of also the S<sub>3</sub> state; this provides further support for the previously suggested O–O bond formation mechanism, with an attack by an oxyl radical, bound to Mn1, on a μ-oxo-ligand bound between Mn3 and Mn4 (4, 12, 13).

**ACKNOWLEDGMENTS.** We thank the Swedish National Infrastructure for Computing for providing computer time. This work was generously supported by the Knut and Alice Wallenberg Foundation and by grants from the Swedish Research Council. X.L. acknowledges support from Beijing Normal University (Grant 2014NT10) and National Science Foundation of China (Grant 21131003).

1. Ferreira KN, Iverson TM, Maghlaoui K, Barber J, Iwata S (2004) Architecture of the photosynthetic oxygen-evolving center. *Science* 303(5665):1831–1838.
2. Loll B, Kern J, Saenger W, Zouni A, Biesiadka J (2005) Towards complete cofactor arrangement in the 3.0 Å resolution structure of photosystem II. *Nature* 438(7070):1040–1044.
3. Guskov A, et al. (2009) Cyanobacterial photosystem II at 2.9-Å resolution and the role of quinones, lipids, channels and chloride. *Nat Struct Mol Biol* 16(3):334–342.
4. Siegbahn PEM (2006) O–O bond formation in the S(4) state of the oxygen-evolving complex in photosystem II. *Chemistry* 12(36):9217–9227.
5. Siegbahn PEM (2008) A structure-consistent mechanism for dioxygen formation in photosystem II. *Chemistry* 14(27):8290–8302.
6. Umena Y, Kawakami K, Shen JR, Kamiya N (2011) Crystal structure of oxygen-evolving photosystem II at a resolution of 1.9 Å. *Nature* 473(7345):55–60.
7. Grundmeier A, Dau H (2012) Structural models of the manganese complex of photosystem II and mechanistic implications. *Biochim Biophys Acta* 1817(1):88–105.
8. Lubner S, et al. (2011) S1-state model of the O<sub>2</sub>-evolving complex of photosystem II. *Biochemistry* 50(29):6308–6311.
9. Galstyan A, Robertazzi A, Knapp EW (2012) Oxygen-evolving Mn cluster in photosystem II: The protonation pattern and oxidation state in the high-resolution crystal structure. *J Am Chem Soc* 134(17):7442–7449.
10. Ames W, et al. (2011) Theoretical evaluation of structural models of the S<sub>2</sub> state in the oxygen evolving complex of Photosystem II: Protonation states and magnetic interactions. *J Am Chem Soc* 133(49):19743–19757.
11. Siegbahn PEM (2011) The effect of backbone constraints: The case of water oxidation by the oxygen-evolving complex in PSII. *ChemPhysChem* 12(17):3274–3280.
12. Siegbahn PEM (2013) Water oxidation mechanism in photosystem II, including oxidations, proton release pathways, O–O bond formation and O<sub>2</sub> release. *Biochim Biophys Acta* 1827(8–9):1003–1019.
13. Siegbahn PEM (2009) Structures and energetics for O<sub>2</sub> formation in photosystem II. *Acc Chem Res* 42(12):1871–1880.
14. Rapatskiy L, et al. (2012) Detection of the water-binding sites of the oxygen-evolving complex of Photosystem II using W-band 17O electron–electron double resonance-detected NMR spectroscopy. *J Am Chem Soc* 134(40):16619–16634.
15. Cox N, et al. (2014) Photosynthesis. Electronic structure of the oxygen-evolving complex in photosystem II prior to O–O bond formation. *Science* 345(6198):804–808.
16. Siegbahn PEM (2012) Mechanisms for proton release during water oxidation in the S<sub>2</sub> to S<sub>3</sub> and S<sub>3</sub> to S<sub>4</sub> transitions in photosystem II. *Phys Chem Chem Phys* 14(14):4849–4856.
17. Yano J, et al. (2005) High-resolution Mn EXAFS of the oxygen-evolving complex in photosystem II: Structural implications for the Mn<sub>4</sub>Ca cluster. *J Am Chem Soc* 127(43):14974–14975.
18. Robblee JH, et al. (2002) The Mn cluster in the S(0) state of the oxygen-evolving complex of photosystem II studied by EXAFS spectroscopy: Are there three Di-μ-oxo-bridged Mn(2) moieties in the tetranuclear Mn complex? *J Am Chem Soc* 124(25):7459–7471.
19. Pushkar Y, et al. (2007) Structure and orientation of the Mn<sub>4</sub>Ca cluster in plant photosystem II membranes studied by polarized range-extended X-ray absorption spectroscopy. *J Biol Chem* 282(10):7198–7208.
20. Haumann M, et al. (2005) Structural and oxidation state changes of the photosystem II manganese complex in four transitions of the water oxidation cycle (S<sub>0</sub> → S<sub>1</sub>, S<sub>1</sub> → S<sub>2</sub>, S<sub>2</sub> → S<sub>3</sub>, and S<sub>3,4</sub> → S<sub>0</sub>) characterized by X-ray absorption spectroscopy at 20 K and room temperature. *Biochemistry* 44(6):1894–1908.
21. Glöckner C, et al. (2013) Structural changes of the oxygen-evolving complex in photosystem II during the catalytic cycle. *J Biol Chem* 288(31):22607–22620.
22. Li X, Sproviero EM, Ryde U, Batista VS, Chen G (2013) Theoretical EXAFS studies of a model of the oxygen-evolving complex of photosystem II obtained with the quantum cluster approach. *Int J Quantum Chem* 113(4):474–478.
23. Hsiao YW, Tao Y, Shokes JE, Scott RA, Ryde U (2006) EXAFS structure refinement supplemented by computational chemistry. *Phys Rev B* 74:214101.
24. Ryde U, Hsiao YW, Rulisek L, Solomon EI (2007) Identification of the peroxy adduct in multicopper oxidases by a combination of computational chemistry and extended X-ray absorption fine-structure measurements. *J Am Chem Soc* 129(4):726–727.
25. Fonda E, Michalowicz A, Randaccio L, Tauzher G, Vlaic G (2001) EXAFS data analysis of vitamin B12 model compounds—a methodological study. *Eur J Inorg Chem* 2001(5):1269–1278.
26. Hsiao YW, Ryde U (2006) Interpretation of EXAFS spectra for sitting-atop complexes with the help of computational methods. *Inorg Chim Acta* 359(4):1081–1092.
27. Gatt P, Stranger R, Pace RJ (2011) Application of computational chemistry to understanding the structure and mechanism of the Mn catalytic site in photosystem II—a review. *J Photochem Photobiol B* 104(1–2):80–93.
28. Blomberg MRA, Borowski T, Himof F, Liao RZ, Siegbahn PEM (2014) Quantum chemical studies of mechanisms for metalloenzymes. *Chem Rev* 114(7):3601–3658.
29. Becke AD (1993) Density-functional thermochemistry. III. The role of exact exchange. *J Chem Phys* 98:5648–5652.
30. Perdew JP (1986) Density-functional approximation for the correlation energy of the inhomogeneous electron gas. *Phys Rev B Condens Matter* 33(12):8822–8824.
31. Siegbahn PEM, Blomberg MRA (2013) Energy diagrams for water oxidation in photosystem II using different density functionals. *J Chem Theory Comput* 10(1):268–272.
32. Pantazis DA, Ames W, Cox N, Lubitz W, Neese F (2012) Two interconvertible structures that explain the spectroscopic properties of the oxygen-evolving complex of photosystem II in the S<sub>2</sub> state. *Angew Chem Int Ed Engl* 51(39):9935–9940.
33. Messinger J, et al. (2001) Absence of Mn-centered oxidation in the S(2) → S(3) transition: Implications for the mechanism of photosynthetic water oxidation. *J Am Chem Soc* 123(32):7804–7820.
34. Yachandra VK, Sauer K, Klein MP (1996) Manganese cluster in photosynthesis: Where plants oxidize water to dioxygen. *Chem Rev* 96(7):2927–2950.
35. Messinger J (2004) Evaluation of different mechanistic proposals for water oxidation in photosynthesis on the basis of Mn<sub>4</sub>O<sub>2</sub>Ca structures for the catalytic site and spectroscopic data. *Phys Chem Chem Phys* 6:4764–4771.
36. Iuzzolino L, Dittmer J, Dörner W, Meyer-Klaucke W, Dau H (1998) X-ray absorption spectroscopy on layered photosystem II membrane particles suggests manganese-centered oxidation of the oxygen-evolving complex for the S<sub>0</sub>–S<sub>1</sub>, S<sub>1</sub>–S<sub>2</sub>, and S<sub>2</sub>–S<sub>3</sub> transitions of the water oxidation cycle. *Biochemistry* 37(49):17112–17119.
37. Brena B, Siegbahn PEM, Ågren H (2012) Modeling near-edge fine structure X-ray spectra of the manganese catalytic site for water oxidation in photosystem II. *J Am Chem Soc* 134(41):17157–17167.
38. Klaus A, Haumann M, Dau H (2012) Alternating electron and proton transfer steps in photosynthetic water oxidation. *Proc Natl Acad Sci USA* 109(40):16035–16040.
39. Siegbahn PEM (2001) Modeling aspects of mechanisms for reactions catalyzed by metalloenzymes. *J Comput Chem* 22(14):1634–1645.